Nanotube nucleation versus carbon-catalyst adhesion–Probed by molecular dynamics simulations

Morgana A. Ribas,[1] Feng Ding,[1,2] Perla B. Balbuena,[3] and Boris I. Yakobson[1,a)]
[1]*Department of Mechanical Engineering and Materials Science, Department of Chemistry, Rice University, Houston, Texas 77005, USA*
[2]*Institute of Textile and Clothing, Hong Kong Polytechnic University, Hong Kong, China*
[3]*Department of Chemical Engineering, Texas A&M University, College Station, Texas 77843, USA*

(Received 13 August 2009; accepted 2 November 2009; published online 8 December 2009)

Catalytic nucleation of carbon nanotubes (CNTs) remains a challenge for the theory: Which factors and forces decide if the gathering sp^2-network of atoms will adhere to the catalyst particle and fully cover it or the graphitic cap will liberate itself to extend into a hollow filament? This intimate mechanism cannot be seen in experiment, yet it can be investigated through comprehensive molecular dynamics. We systematically vary the adhesion strength (W_{ad}) of the graphitic cap to the catalyst and temperature T (and C diffusion rate). Observations allow us to build a statistically representative map of CNT nucleation and define the conditions for growth or metal encapsulation in a fullerene-shell (catalyst poisoning). It shows clearly that weak W_{ad}, sufficient thermal kinetic energy (high T) or fast C diffusion favor the CNT nucleation. In particular, below 600 K carbon-diffusion on the catalyst surface limits the growth, but at higher T it fully depends on cap lift-off. Informed choice of parameters allowed us to obtain the longest simulated nanotube structures. The study reveals a means of designing the catalyst for better CNT synthesis, potentially at desirably low temperatures. © *2009 American Institute of Physics*. [doi:10.1063/1.3266947]

I. INTRODUCTION

Despite key experimental advances to produce longer carbon nanotubes (CNTs), [1,2] with more uniform diameter distribution[3–6] and at lower temperatures,[7–10] the mechanism of single-wall carbon nanotubes (SWNT) growth at the atomic level is far from being completely understood. We still do not know how to fully control SWNT growth or even if such control can be achieved. Meanwhile, complete utilization of SWNT remarkable electronic properties awaits this scientific and technological achievement.

Experimentally, transmission electron microscopy *in situ* observations allow one to see the nucleation and growth of SWNT in some detail.[11–13] However, processes such as feedstock decomposition on catalyst surface, C diffusion on or through the catalyst and C incorporation into the SWNT wall cannot be seen directly. Fortunately, these details, which are key parts of the SWNT growth mechanism, can be explored using molecular dynamics (MD) simulations.[14–16] Recently developed dislocation theory of nanotube growth[17] transforms the principles of crystal step-flow to the lower-dimension of a tube edge; it enables quantitative predictions of growth rate of individual SWNT, yet does not address at all the complementary and important stages of nucleation.

The cap lift-off versus catalyst encapsulation is the "to be or not" question in the SWNT formation and has been studied extensively by theoretical methods, including *ab initio* methods,[18–20] tight-binding MD (TBMD)[21,22] or tight-binding Monte Carlo[23,24] simulations, and classical MD simulations.[14–16,25] *Ab initio* based MD is the most time consuming method and is only able to simulate small carbon-metal systems for a few picoseconds.[18–20] TBMD is an intermediary expensive method; it is hundreds of times faster than *ab initio* DFT based MD and can be used to simulate CNT growth in a reasonable time period (e.g., 100 ps).[21,22] Classical MD simulations are two and three orders of magnitude faster than TBMD and therefore can be applied to large systems (up to 1000 atoms) and perform very long trajectories of up to 100 ns.[10,16]

In the often referred to phenomenological vapor-liquid-solid model, a complete CNT growth process is divided into three successive stages: Cap nucleation, cap lift-off as a short SWNT, and SWNT lengthening.[12,26–28] Detrimental to growth, catalyst encapsulation prevents feedstock from accessing the catalyst, a phenomenon known as catalyst poisoning, hindering cap lift-off and growth. Thus avoiding catalyst encapsulation during both nucleation and growth stages is critical for SWNT growth. Here we report an exhaustive theoretical study aimed to elucidate the role of work of adhesion (W_{ad}) between graphitic cap and catalyst, temperature, and C diffusion in catalyst encapsulation (or poisoning) at the nucleation stage. Statistics over more than 500 MD simulations clearly show that the work of adhesion controls the high temperature region, in which the C mobility is sufficiently high, while slow C diffusion may result in an encapsulated catalyst at low temperature. Also our analysis suggests that room temperature growth of CNT is possible if the work of adhesion could be significantly reduced through careful selection of the catalyst.

a)Electronic mail: biy@rice.edu.

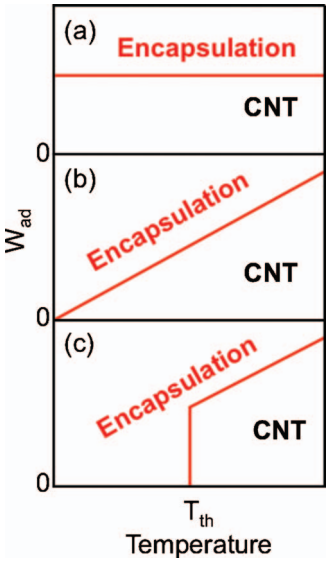

FIG. 1. Temperature dependence of SWNT growth/catalyst encapsulation as a function of work of adhesion has distinct characteristics for (a) curvature-energy, (b) thermal decohesion, and (c) fast C diffusion models (see text for details).

II. THEORETICAL ANALYSIS

Until now, three different aspects of the cap lift-off versus catalyst encapsulation have been distinguished and discussed: Adhesion versus curvature energy balance,[29] decohesion by thermal kinetic energy model,[30,31] and requirement of fast C diffusion. In order to compare and evaluate these three models we have constructed diagrams showing the temperature dependence of catalyst encapsulation as a function of work of adhesion, W_{ad} (Fig. 1).

A. Curvature energy model

This model considers the energy difference between a growing tube and an encapsulated catalyst.[29] For small catalysts (diameter smaller than 3 nm), a growing SWNT is energetically favorable if the work of adhesion between the fullerene and catalyst particle is less than the curvature energy difference between the SWNT and the fullerene.

$$W_{ad,cF} < E_{cF} - E_{cT}, \tag{1}$$

where W_{ad} is the work of adhesion, and E_{cF} and E_{cT} are curvature energy of the fullerene and SWNT, respectively. Inequality (1) shows that catalyst encapsulation happens only if the surrounding fullerene, which has larger curvature energy than that a SWNT of same diameter, is strongly attracted by the catalyst particle. According to this inequality, for catalysts with diameter larger than 3 nm, a graphitic encapsulation is energetically more favorable. This model correctly explains the narrow diameter distribution of SWNT grown in floating catalyst experiments (e.g., arc discharge, laser ablation, and HiPco). However, it does not apply to cases of a catalyst sitting on a substrate, in which a strong subtract-catalyst interaction could prevent the formation of catalyst encapsulation. In general, the curvature energy model predicts that catalyst encapsulation is a function of only catalyst diameter and work of adhesion [Fig. 1(a)].

B. Thermal decohesion model

A strong argument against the above mechanistic energy model was that the thermal fluctuations[30,31] must play a role (and even thermodynamic theory is not fully applicable because the kinetics must be considered in the nonequilibrium process of CNT growth[17,32]). To augment the lack of thermal fluctuations in the curvature energy model, it has been suggested that for a SWNT to grow, it needs thermal kinetic energy sufficient to overcome the work of adhesion between graphene and catalyst.[16,25] To permit the cap lift-off on a catalyst surface during SWNT nucleation stage, a proposed criterion is

$$E_{kin} > W_{ad}, \tag{2}$$

where $E_{kin} \sim k_B T$ is the kinetic energy of a carbon atom on the graphitic cap (k_B is Boltzmann's constant). Such a model was used to estimate the diameter distribution of the SWNT growth in laser ablation or arc discharge experiments.[31] In sharp contrast to the curvature energy model, this model shows that the cap lifting-off is independent of the catalyst diameter but strongly dependent on the SWNT growth temperature [Fig. 1(b)].

C. Requirement of fast C diffusion

Recent MD simulations[14,25] clearly show that sufficiently rapid C diffusion is required to avoid the catalyst encapsulation. During SWNT growth, all deposited carbon atoms, which may arrive at the catalyst surface randomly due to feedstock decomposition, must incorporate into the SWNT wall through the SWNT-catalyst contact circle. Thus, if the C mobility is not sufficient, the slowly moving C atoms may nucleate into graphitic islands or caps around the catalyst surface and eventually encapsulate the whole catalyst. This encapsulation due to lack of C mobility means that there is a threshold temperature T_{th}, which depends on the C deposition rate, and below which the catalyst encapsulation is inevitable. MD simulations[25] also show that temperatures above T_{th} are required for the growth energy to overcome the work of adhesion [Fig. 1(c)]

$$T > T_{th}. \tag{3}$$

All three diagrams in Fig. 1 are distinct and even seem to disagree, which is not surprising because the corresponding models emphasize different factors. The curvature energy model is temperature independent, whereas the thermal decohesion model shows a W_{ad} on the encapsulation-CNT boundary as proportional to T. Experimentally, although SWNT growth dependence on temperature was well studied, it is not possible to identify precisely the role of kinetic energy or the work of adhesion on it.

Here we study the catalyst encapsulation as a function of W_{ad}, temperature, and consequently the C diffusion rate, by classical MD simulations. Compared with the *ab initio* method or tight-binding approximation based MD, the potential energy surface (PES) of classical MD simulation is considered less accurate, although it permits to run trajectories many orders of magnitude longer. Availability of long enough simulation time is critical to reasonably simulate

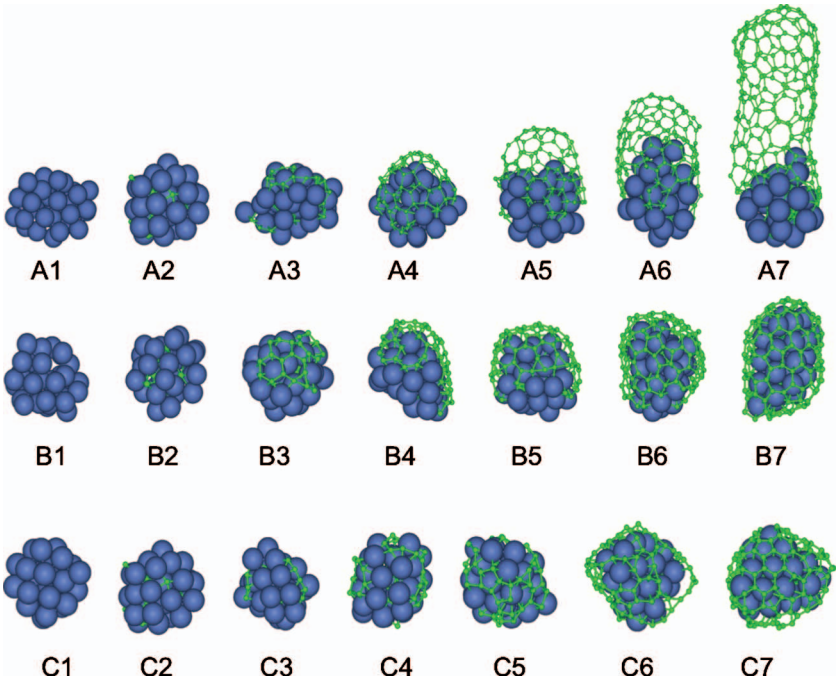

FIG. 2. At 1000 K and lower W_{ad}(~0.04 eV/C) C nucleates (A2–A3) on the catalyst surface forming a graphitic cap (A4) that lifts off (A5) and grows further into a SWNT (A6–A7). A cap forms in the same way at 1000 K but higher W_{ad}(~0.2 eV/C) (B1–B4); however, it does not lift-off and grows until it encapsulates the entire catalyst surface (B5–B7) and thus deactivates it. At 200 K and lower W_{ad}(~0.04 eV/C) the metal catalyst encapsulates due to extremely slow C diffusion (C1–C7), when initially sparse C-network gradually thickens, to become impermeable for further carbon feedstock.

SWNT growth process. Another advantage of the classical PES is that all the parameters are adjustable, which allows us to gain insight into the role of a specific parameter. For example, recently Ding *et al.*[33] studied how a catalyst would maintain an open end of a growing SWNT by varying the bond strength between the open end and the catalyst.

III. POTENTIAL ENERGY SURFACE AND COMPUTATIONAL DETAILS

In this study, we use a classical PES in order to run a sufficient number of long time MD trajectories that provide statistical results. The PES used in our simulations was based on a potential (developed at Texas A&M University) which was previously successfully used to simulate the catalytic growth of SWNT.[15,34] A detailed description is available in Ref. 35. For this study, an important characteristic of this potential is the possibility to vary the interaction forces between sp^2 hybrid C and the metal cluster. We use this particular characteristic to gradually tune the work of adhesion between graphene and metal cluster (0.0 to ~0.3 eV/C). For details of varying the work of adhesion, see supporting materials I.[36] In this way, we are able to study the role of W_{ad} in the nucleation of SWNT by classical MD simulation.

For each simulation, a M_{32} cluster (Fig. 2, A1) is positioned in a periodic box (size $6\times6\times6$ nm^3) that is filled with precursor gas (density kept constant at 0.04 molecule nm^{-3}). In resemblance with the early stages of CNT growth, where carbon atoms dissolve into a catalyst and then precipitate on its surface before nucleation,[16,37,38] the PES considers a metal-carbon distance (calculated by DFT during its development[35]). Once an "uncatalyzed" C atom is close enough to a catalyst atom (metal-carbon distance less than 0.18 nm), it is "catalyzed" into a normal C atom (i.e., its stronger interaction with metal is switched on), mimicking carbon feedstock decomposition in CVD CNT growth. Atomic interactions (C–C, C–Ni, and Ni–Ni) are calculated with an earlier developed potential.[35] The choice of relatively small metal particles allows us to completely simulate a trajectory in a reasonable computational time using only one CPU; a few days for most of the simulations (the longest tube showed later in Fig. 5 was completed in about a month). In this way we are able to carry out the several hundreds of trajectories that are part of this study. Although encapsulation may occur at different conditions, as a combination of temperature and work of adhesion between the graphitic structure and the catalyst, we expect a similar dependence for catalyst particles of different sizes.

To study the competition of tubular structure versus encapsulated catalyst as a function of temperature and W_{ad}, we perform MD simulations for a temperature range between 200 and 1400 K, at 200 K increments. For each temperature we vary W_{ad} from 0 to 0.3 eV/C. In order to obtain more representative and convincing results, five runs are performed for each T and level of W_{ad}. In total, more than 500 MD simulations were carried out for this study. The Verlet algorithm[39,40] is used to integrate the equations of motion at a small time step of 0.5 fs.

IV. RESULTS AND DISCUSSION

Figure 2 (A1–A7) depicts a SWNT growth starting from a pure M_{32} cluster at 1000 K and with W_{ad}=0.04 eV/C. The SWNT growth process is generally close to that shown in previous publications of Ding *et al.*:[16,37,38] At early stages carbon atoms dissolve into a catalyst (A1 → A2) and then

precipitate to the catalyst surface (A2) to nucleate into carbon chains and polygons (A3). Eventually a carbon island or carbon cap is formed (A4). A key step toward a SWNT formation is the lift-off of the graphitic cap from the catalyst surface (A4, A5). The SWNT grows longer and longer (A5 $\rightarrow$A6$\rightarrow$A7) in a repeatable manner. The resulting SWNT has roughly the same diameter as the catalyst particle ($\sim$1 nm), as often observed experimentally.[6,41,42] Unfortunately, as in previously simulated nanotubes, there is a number of defects (pentagons and heptagons) which frequently appear on the tube wall in such a way that we are not able to assign it a pair of (n,m) chiral indexes.[14,16,18,21,22] Note that this may be a consequence of the limited simulation time when compared to real experiments. The initial nucleation stage of the simulation with a large W_{ad}($\sim$0.2 eV/C), Fig. 2 (B1–B4), is almost exactly the same as shown above, Fig. 2 (A1–A4), but here the cap lift-off does not occur. Instead, the graphitic cap grows larger and larger until it covers the whole surface of the catalyst (Fig. 2, B4$\rightarrow$B5$\rightarrow$B6$\rightarrow$B7). It is important to note that the catalyst surface that is not covered with a graphitic cap is almost totally free of C atoms, a result that is explained as a consequence of the reduction of dissolved carbon concentration and fast carbon diffusion.[25,38] Figure 2(c) shows another simulation at temperature of 200 K and with lower $W_{ad}\sim$0.04 eV/C. Although the early nucleation stage (C atoms dissolved in the catalyst) resembles the simulations performed at high temperature, they differ significantly, as is shown below. Because of the low temperature, C diffusion is extremely slow and most of the catalyzed C atoms just stay on the initial position and a catalyzed C atom can interact only with those around it. As a consequence, C chains and small islands may form everywhere around the catalyst surface (C3, C4). Additional catalyzed carbon atoms connect these islands to form a low quality C network around the catalyst surface (C5, C6). This network becomes a full encapsulated graphene layer around the catalyst after its holes are repaired (C6$\rightarrow$C7). The difference in encapsulation processes at low and high temperature clearly shows an important role of C diffusion for SWNT growth.

A strong correlation between catalyst encapsulation and W_{ad} is clearly depicted. Figure 3 shows the simulation results at 1000 K and supporting materials II (Ref. 36) includes simulations at other temperatures. At lesser values of work of adhesion ($W_{ad}<130$ meV/C), SWNT formation appears in all MD simulations. However, catalyst encapsulation starts to happen at intermediate levels of work of adhesion ($130<W_{ad}<170$ meV/C), to finally become inevitable at higher work of adhesion values ($W_{ad}>170$ meV/C). Roughly, the transition from SWNT to catalyst encapsulation occurs at $W_{ad}\sim$150 meV/C or $\sim$1.7 k_BT, which is qualitatively in agreement with the thermal decohesion model [Eq. (2)]. Comparing the same simulation results to the curvature energy model, we observe that curvature energy for the SWNT is $E_{cSWNT}(D)=C/D^2$, $C=0.08$ (eV nm^2/atom), whereas it doubles for the fullerenelike encapsulated catalyst, $E_{cF}(D)=2E_{cSWNT}(D)$. Since the diameter of the catalyst is $\sim$1 nm, the curvature energy difference between an fullerenelike encapsulated catalyst and a SWNT is about $\Delta E_c=80$ meV/C,

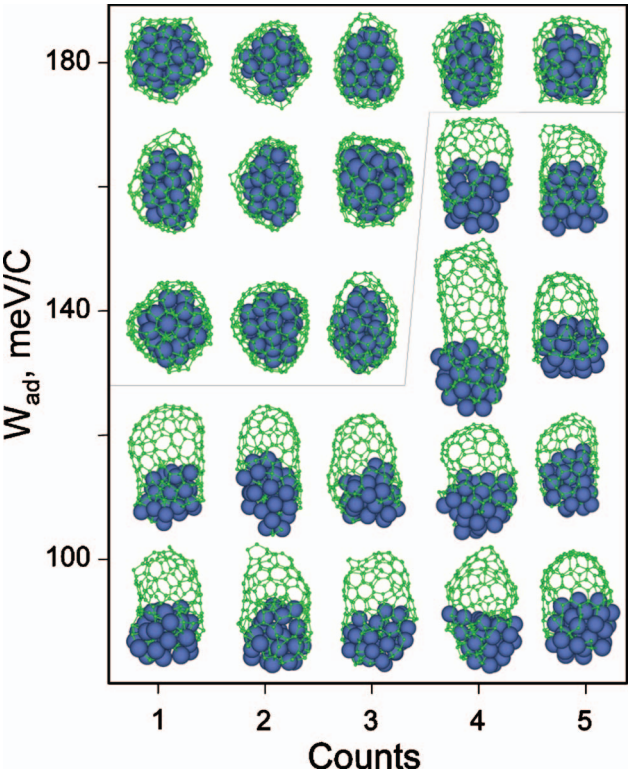

FIG. 3. SWNT growth and catalyst encapsulation are strongly dependent on work of adhesion. Here an example at T=1000 K including all five simulations, repeated for each value of W_{ad}. (Thin line separates the incidents of encapsulation from those with lift-off.)

which seems to be only half of the critical work of adhesion according to the curvature energy model. However, considering the high simulation temperature and the low structural quality of the SWNTs, this disagreement is still in the range of error.

Additionally, all MD simulations that we have performed, at different temperatures and levels of W_{ad} values (shown in Fig. 3 and in the supporting materials),[36] exhibit similar dependence on the work of adhesion [Fig. 4(a)] and strongly support the idea that the work of adhesion controls the catalyst encapsulation. Statistical plots of these numerical experiments are presented as a diagram of SWNT formation versus catalyst encapsulation [Fig. 4(b)] that clearly shows two distinct regions. At higher temperatures, W_{ad} linearly depends on temperature. This dependence on temperature means that to lift-off the graphitic cap from the catalyst surface, higher temperatures are required at larger values of work of adhesion. This trend is in agreement with most experimental observations:[4,29,43] SWNTs require high temperatures for growth, whereas catalysts are encapsulated at lower temperatures. The slope of the threshold temperature is lower than that predicted by the thermal decohesion model, which means that sufficient kinetic energy is not the only cause for graphitic cap lift-off. The change in curvature energy, formation energy of the required pentagons, and edge tension around the cap should also be carefully considered. These considerations were partially included in the model proposed by Kuznetsov *et al.*[44] but a more detailed discussion is beyond the scope of this paper.

Catalyst encapsulation dependence is very different at

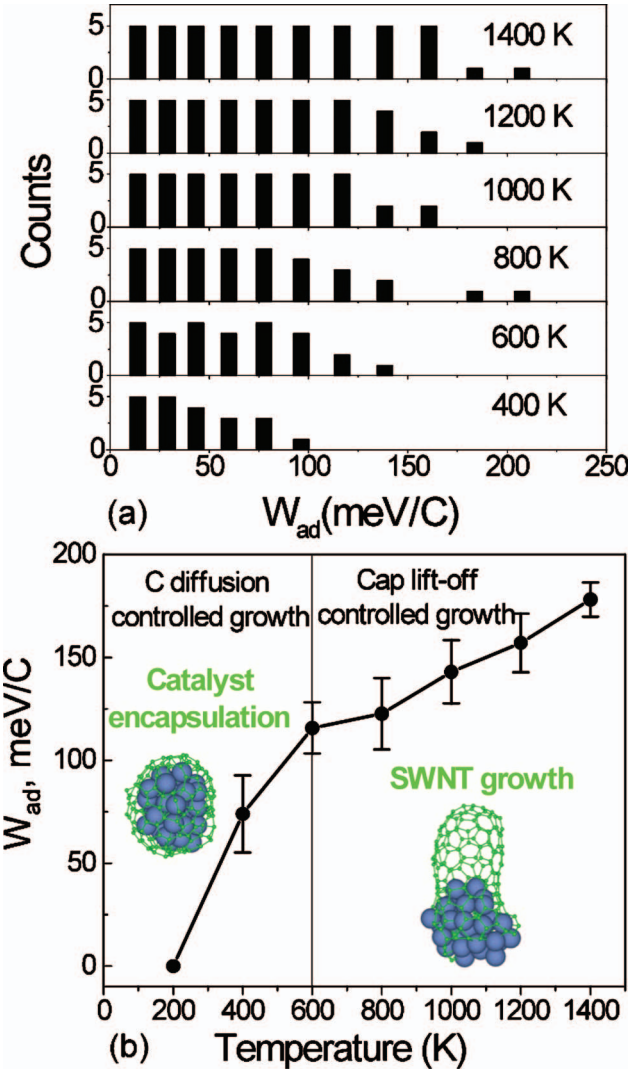

FIG. 4. (a) Statistical plots of the number of tubes (counts 0 to 5) at different levels of W_{ad}, from 400 to 1400 K, show two distinct regions. (b) At temperatures higher than 600 K SWNT growth is nearly temperature independent, whereas at lower temperatures (<600 K) it is strongly temperature dependent, as limited C diffusion hinders cap lift-off and growth.

$T < 600$ K; it strongly depends on temperature. At very low temperature, for example at 200 K as shown in Fig. 2, C1–C7, the catalyst is in a solid shape, which limits the diffusion of C atoms both on its surface and across its body. This lack of diffusion hinders the transport of catalyzed carbon atoms to the growing cap or SWNT and results in catalyst encapsulation by a nucleated graphitic structure around its surface [Fig. 2(c)]. As a consequence, we have never observed any tubular structure to be formed at this very low temperature level, even at a minimum work of adhesion. Thereby, at low temperature range ($T < 600$ K) there is a strong temperature dependence, because its reduction will significantly reduce the carbon diffusion coefficient, $D \sim \exp(-E_D/k_BT)$, where E_D is the diffusion barrier.

Here one can ask: What is the lowest temperature at which a SWNT can grow? Early on, motivated by SWNT production from arc discharge and laser ablation experiments, it was believed that a very high temperature is required to grow SWNTs, mainly because of the high melting point of carbon materials.[28,45,46] Gradually, the lowest SWNT growth temperature was reduced below 1000 °C,[8–10] until being recently reported as 350 °C.[7] Experimentally, it was shown that low SWNT growth temperature is limited by the feedstock decomposition, thus being sensitively dependent on the type of carbon feedstock.[47] From the point of view of graphitic cap lift-off, we understand that the lowest SWNT growth temperature must be associated with work of adhesion and diffusion of catalyzed C atoms. Ideally, as shown in Fig. 4, one can find the lowest SWNT growth temperature for a given catalyst with known constant work of adhesion. The measurement and calculation of W_{ad} is still a big challenge and the accuracy of the present data is very low. The Ni-C interaction energy in a nanotube was estimated to be between 10 and 1000 meV.[48] Even the data obtained from state of the art *ab initio* calculation are widely distributed within a large range (Table I, calculation methods described in the supporting materials).[36] Thus, we could not apply such analysis to obtain the lowest SWNT growth lift-off temperature of a given catalyst (e.g., Fe, Co, Ni, Au, and Cu). However, we expect it to be obtained in the future, based on the information contained in Fig. 4, through more accurate measurement or calculation of W_{ad}.

TABLE I. Ni (111)—graphene binding energy (E_b) and equilibrium distance (d_{GM}) calculated using different pseudopotentials. Details of the *ab initio* calculations are shown in supporting material III (Ref. 36).

Ni (111) stacking	Pseudopotential	E_b (meV)	d_{GM} (Å)
AC	PAW-PBE	13.65	2.12
	PAW-LDA	290.44	1.95
	Ultrasoft-LDA	196.38	1.96
BC	PAW-PBE	40.29	3.85
	PAW-LDA	78.29	3.34
	Ultrasoft-LDA	38.19	3.30

On the other hand, considering the reported lowest SWNT growth temperature on iron (350 °C), we can estimate that the work of adhesion of an iron catalyst must be less than ~120 meV/C. In fact, our calculated results show that SWNT growth near room temperature (e.g., 273 K) is possible at very low level of work of adhesion $W_{ad} < 50$ meV/C. Of course the presented MD simulations completely neglect the effects of feedstock conversion and catalyst activity, the role of buffer gas and substrate, which should be accounted for prior to real experiments (e.g., Ref. 49) analysis. Feedstock-decomposition and C diffusion may prohibit the overall synthesis at low temperature and should be studied separately in future. Although these aspects remain oversimplified in present simulations, our findings strongly encourage search of catalysts with low W_{ad}(<50 meV/C) and sufficient C diffusion, in order to achieve lower SWNT growth temperatures.

The relationship between W_{ad} and T [Fig. 4(b)], allows us to choose these parameters and obtain, as far as we know, the longest SWNT produced in any MD simulation up to date. At 600 K and $W_{ad}=50$ meV, we begin at relatively low carbon-gas density (0.02 molecule nm^{-3}), and initially obtain a tube of ~1.2 nm in length (comparable to reported

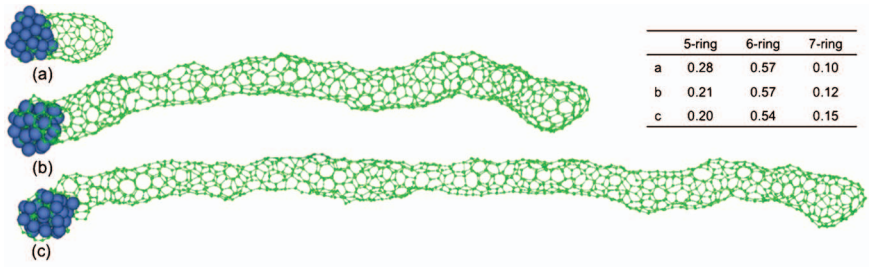

FIG. 5. Choosing the parameters based on Fig. 4, we obtain the longest SWNT, here at 600 K and W_{ad}=50 meV/C. (a) ~1.2 nm in length after 10 ns at 0.02 molecule nm^{-3}, (b) ~8.2 nm after 20.5 ns, and (c) ~13 nm after 27 ns, both [(b) and (c)] at 0.04 molecule nm^{-3}. Inset: Proportion of pentagons, hexagons, and heptagons at different simulation times.

earlier[15,25]). Moreover, we successfully continue at somewhat higher precursor gas density (0.04 molecule nm^{-3}), to accelerate the growth. Figures 5(b) and 5(c) show the SWNT as long as ~8.2 nm and then even ~13 nm, without detectable changes in quality (the proportion of hexagons is shown in the inset in Fig. 5). Although the quality requires further improvement, just the fact of steady uninterrupted growth within reasonable simulation times represents a significant step of achieving realistic computational modeling.

V. CONCLUSIONS

Understanding the SWNT cap lift-off is a crucial part of CNT growth research. Until now, all three available models had different predictions on what is the driving force behind cap lift-off. Through MD simulations we introduce here a more comprehensive picture composed of two distinct regions: (1) High temperature (>600 K), where catalyst encapsulation depends on work of adhesion and (2) low temperature (<600 K), or strongly temperature dependent, where limited C diffusion hinders cap localization and lift-off for growth. Our simulations also show that SWNT growth is strongly dependent on work of adhesion and C diffusion at very low temperatures (e.g., 273 K). Based on our analysis, it is suggested that experimental low SWNT growth temperatures can be achieved through use of catalysts with low work of adhesion value. This is critically important not only from general process efficiency point of view but especially for possible *in situ* growth for nanoelectronics applications.

ACKNOWLEDGMENTS

This work was supported by the National Science Foundation, Grant No. CBET-0731246, and partially by the Honda Research Institute and the Air Force Research Laboratory. P.B.B. acknowledges support by the Department of Energy, Basic Energy Sciences, Grant. No. DE-FG02-06ER15836. M.A.R. was partially supported by the Roberto Rocca Fellowship.

[1] L. X. Zheng, M. J. O'Connell, S. K. Doorn, X. Z. Liao, Y. H. Zhao, E. A. Akhadov, M. A. Hoffbauer, B. J. Roop, Q. X. Jia, R. C. Dye, D. E. Peterson, S. M. Huang, J. Liu, and Y. T. Zhu, Nature Mater. **3**, 673 (2004).
[2] Z. Yang, X. Chen, H. Nie, K. Zhang, W. Li, B. Yi, and L. Xu, Nanotechnology **19**, 085606 (2008).
[3] A. Thess, R. Lee, P. Nikolaev, H. Dai, P. Petit, J. Robert, C. Xu, Y. H. Lee, S. G. Kim, A. G. Rinzler, D. T. Colbert, G. E. Scuseria, D. Tomanek, J. E. Fischer, and R. E. Smalley, Science **273**, 483 (1996).
[4] H. Kataura, Y. Kumazawa, Y. Maniwa, Y. Ohtsuka, R. Sen, S. Suzuki, and Y. Achiba, Carbon **38**, 1691 (2000).
[5] S. M. Bachilo, L. Balzano, J. E. Herrera, F. Pompeo, D. E. Resasco, and R. B. Weisman, J. Am. Chem. Soc. **125**, 11186 (2003).
[6] C. L. Cheung, A. Kurtz, H. Park, and C. M. Lieber, J. Phys. Chem. B **106**, 2429 (2002).
[7] M. Cantoro, S. Hofmann, S. Pisana, V. Scardaci, A. Parvez, C. Ducati, A. C. Ferrari, A. M. Blackburn, K. Y. Wang, and J. Robertson, Nano Lett. **6**, 1107 (2006).
[8] E. J. Bae, Y.-S. Min, D. Kang, J.-H. Ko, and W. Park, Chem. Mater. **17**, 5141 (2005).
[9] H. Liao and J. H. Hafner, J. Phys. Chem. B **108**, 6941 (2004).
[10] S. Maruyama, R. Kojima, Y. Miyauchi, S. Chiashi, and M. Kohno, Chem. Phys. Lett. **360**, 229 (2002).
[11] S. Helveg, C. Lopez-Cartes, J. Sehested, P. L. Hansen, B. S. Clausen, J. R. Rostrup-Nielsen, F. Abild-Pedersen, and J. K. Norskov, Nature (London) **427**, 426 (2004).
[12] J. A. Rodríguez-Manzo, M. Terrones, H. Terrones, H. W. Kroto, L. Sun, and F. Banhart, Nat. Nanotechnol. **2**, 307 (2007).
[13] H. Yoshida, S. Takeda, T. Uchiyama, H. Kohno, and Y. Homma, Nano Lett. **8**, 2082 (2008).
[14] Y. Shibuta and S. Maruyama, Chem. Phys. Lett. **382**, 381 (2003).
[15] J. Zhao, A. Martinez-Limia, and P. B. Balbuena, Nanotechnology **16**, S575 (2005).
[16] F. Ding, K. Bolton, and A. Rosen, J. Phys. Chem. B **108**, 17369 (2004).
[17] F. Ding, A. R. Harutyunyan, and B. I. Yakobson, Proc. Natl. Acad. Sci. U.S.A. **106**, 2506 (2009).
[18] J.-Y. Raty, F. Gygi, and G. Galli, Phys. Rev. Lett. **95**, 096103 (2005).
[19] X. Fan, R. Buczko, A. A. Puretzky, D. B. Geohegan, J. Y. Howe, S. T. Pantelides, and S. J. Pennycook, Phys. Rev. Lett. **90**, 145501 (2003).
[20] J. Gavillet, A. Loiseau, C. Journet, F. Willaime, F. Ducastelle, and J. C. Charlier, Phys. Rev. Lett. **87**, 275504 (2001).
[21] Y. Ohta, Y. Okamoto, S. Irle, and K. Morokuma, ACS Nano **2**, 1437 (2008).
[22] Y. Ohta, Y. Okamoto, S. Irle, and K. Morokuma, J. Phys. Chem. C **113**, 159 (2009).
[23] H. Amara, C. Bichara, and F. Ducastelle, Phys. Rev. B **73**, 113404 (2006).
[24] J.-C. Charlier, H. Amara, and P. Lambin, ACS Nano **1**, 202 (2007).
[25] F. Ding, A. Rosen, E. E. B. Campbell, L. K. L. Falk, and K. Bolton, J. Phys. Chem. B **110**, 7666 (2006).
[26] R. S. Wagner and W. C. Ellis, Appl. Phys. Lett. **4**, 89 (1964).
[27] R. T. K. Baker, M. A. Barber, P. S. Harris, F. S. Feates, and R. J. Waite, J. Catal. **26**, 51 (1972).
[28] Y. Saito, Carbon **33**, 979 (1995).
[29] J. H. Hafner, M. J. Bronikowski, B. R. Azamian, P. Nikolaev, A. G. Rinzler, D. T. Colbert, K. A. Smith, and R. E. Smalley, Chem. Phys. Lett. **296**, 195 (1998).
[30] H. Kanzow and A. Ding, Phys. Rev. B **60**, 11180 (1999).
[31] H. Kanzow, C. Lenski, and A. Ding, Phys. Rev. B **63**, 125402 (2001).
[32] W. M. Zhu, H. M. Duan, and K. Bolton, J. Nanosci. Nanotechnol. **9**, 1222 (2009).
[33] F. Ding, P. Larsson, J. A. Larsson, R. Ahuja, H. Duan, A. Rosen, and K. Bolton, Nano Lett. **8**, 463 (2008).
[34] P. B. Balbuena, J. Zhao, S. Huang, Y. Wang, N. Sakulchaicharoen, and D. E. Resasco, J. Nanosci. Nanotechnol. **6**, 1247 (2006).
[35] A. Martinez-Limia, J. Zhao, and P. Balbuena, J. Mol. Model. **13**, 595

(2007).
[36] See EPAPS supplementary material at http://dx.doi.org/10.1063/1.3266947 for details on the methodology used to calculate W_{ad} in the MD trajectories (SM I), all MD simulation results mentioned in this work (SM II), and details on the *ab initio* DFT calculations performed (SM III).
[37] F. Ding, A. Rosen, and K. Bolton, Carbon **43**, 2215 (2005).
[38] F. Ding, A. Rosen, and K. Bolton, Chem. Phys. Lett. **393**, 309 (2004).
[39] L. Verlet, Phys. Rev. **159**, 98 (1967).
[40] L. Verlet, Phys. Rev. **165**, 201 (1968).
[41] H. Dai, A. G. Rinzler, P. Nikolaev, A. Thess, D. T. Colbert, and R. E. Smalley, Chem. Phys. Lett. **260**, 471 (1996).
[42] D. Ciuparu, Y. Chen, S. Lim, G. L. Haller, and L. Pfefferle, J. Phys. Chem. B **108**, 503 (2004).
[43] M. J. Bronikowski, P. A. Willis, D. T. Colbert, K. A. Smith, and R. E. Smalley, J. Vac. Sci. Technol. A **19**, 1800 (2001).
[44] V. L. Kuznetsov, A. N. Usoltseva, A. L. Chuvilin, E. D. Obraztsova, and J.-M. Bonard, Phys. Rev. B **64**, 235401 (2001).
[45] L. Alvarez, T. Guillard, J. L. Sauvajol, G. Flamant, and D. Laplaze, Chem. Phys. Lett. **342**, 7 (2001).
[46] A. R. Harutyunyan, T. Tokune, and E. Mora, Appl. Phys. Lett. **87**, 051919 (2005).
[47] E. Mora, J. M. Pigos, F. Ding, B. I. Yakobson, and A. R. Harutyunyan, J. Am. Chem. Soc. **130**, 11840 (2008).
[48] S. H. Yang, W. H. Shin, J. W. Lee, S. Y. Kim, S. I. Woo, and J. K. Kang, J. Phys. Chem. B **110**, 13941 (2006).
[49] E. Mora and A. R. Harutyunyan, J. Phys. Chem. C **112**, 4805 (2008).